Estuaries Vol. 25, No. 5, p. 916–929 October 2002

Validation of a Fish Farm Waste Resuspension Model by Use of a Particulate Tracer Discharged from a Point Source in a Coastal Environment

CHRIS J. CROMEY*, THOM D. NICKELL, KENNETH D. BLACK, PAUL G. PROVOST, and COLIN R. GRIFFITHS

Scottish Association for Marine Science, Dunstaffnage Marine Laboratory, Oban, Argyll, PA34 4AD, U.K.

ABSTRACT: To validate a resuspension model of particulate material (salmonid farm wastes), a UV fluorescent particle tracer was selected with similar settling characteristics. Tracer was introduced to the seabed (water depth ~30 m) and sediment samples taken on days 0, 3, 10, 17 and 30 to measure the horizontal and vertical distribution of tracer in sediments. A concentric sampling grid was established at radii of 25, 50, 100, 150, 200, 400, 700 and 1,000 m from the source on transects 30° apart. The bulk of the deployed tracer was initially concentrated in an area 25 m radius from the release point; tracer was observed to steadily decrease to zero over a period of 30 days. In a 200 m region measured from the release point in the direction of the residual current, the redeposition of tracer was low. A Lagrangian particle tracking model was validated using these observed data by varying resuspension model parameters within limits to obtain the best agreement between spatial and temporal distributions. The validated model generally gave good predictions of total mass budgets (± 7% of total tracer released), particulary where tracer concentrations were high near the release point. Best fit model parameters (critical erosion shear stress = 0.018 N m^{-2}, erodibility constant = 60 g m^{-2} d^{-1}) are at the low end of reported parameters for coastal resuspension models. Such a low critical erosion shear stress indicates that the frequency of resuspension and deposition events for freshly deposited material is high.

Introduction

Resuspension and redistribution of particulate material from a point source has numerous effects on the total sediment budget of a given area. Erosion of high concentrations of material from close to the point source may result in redeposition of this material at a distance away from the point source, creating depocenters. These areas which act as sinks of particulate material may be transient or more permanent in nature. For areas directly beneath a point source discharging at the surface, an increase in current velocity will result in a reduction of material available for resuspension on the bed. The main causes of this reduction will be both the increased erosion of previously deposited material and increased advection of recently discharged material while settling to the bed. A reduction in current velocity will result in the opposite, reduced erosion of bed material and reduced advection of freshly discharged material from the source. For a point source at the surface that results in high initial deposition of organic material on the bed (e.g., > 1,000 g solids m^{-2} yr^{-1}), these fluctuations in supply and reduction of particulate material are likely to be primary drivers in determining the physical, chemical and biological characteristics of the bed. The oxygen supply associated with the near bed current will also play an important role in regulating chemical and biological characteristics. During periods of low current, the high oxygen demand caused by large deposition events of organic-rich particulates will be compounded by the reduction in oxygen supply associated with the low current (Findlay and Watling 1997). As current speeds increase, supply of oxygen is restored and with resuspension events acting to reduce resuspendable material on the bed, the oxygen demand is lowered.

Compartmentalisation of resuspension models into erosion–transport–deposition–consolidation processes is common practice and examples of validated models are numerous (Partheniades 1965; Uncles et al. 1985; Puls and Sündermann 1990; Teisson 1991; Clarke and Elliot 1998; Cromey et al. 1998). The critical erosion shear stress incorporated into these models is the main driver of resuspension, a resuspension event occurring when this threshold is exceeded. Validation of this parameter is undertaken by varying it within reported limits for the sediment type being modelled to obtain the best fit to field observations. A time and spatially

* Corresponding author; tele: +44 1631 559000; fax: +44 1631 559001; e-mail: chjc@dml.ac.uk.

constant critical shear stress is used, although this is likely to vary with sediment depth (O'Connor and Nicholson 1992), bed characteristics (Velegrakis et al. 1997), sediment size and density (Amos et al. 1997). Resuspension model parameters that have been made functions of the spring–neap cycle have been shown to work for the Firth of Forth (Clarke and Elliot 1998). In this model, as tidal activity is reduced towards the onset of neap tides, the erosion threshold is increased as bed consolidation occurs. As tidal activity increases and slack water periods are reduced, the reduction in consolidation is caused by the magnitude of tidal velocities exceeding the erosion threshold for a sufficient time to lower the consolidation of the bed.

Reported values of the erosion threshold from both modelling and observation vary considerably. Near bed (typically measured at ≈ 1.0–2.5 m above the bottom) critical resuspension speeds (vr) as low as 7 cm s^{-1} have been observed by Washburn et al. (1991) for organic solids discharged from a long sea outfall on the Californian coast. In estuarine models critical resuspension speeds in excess of 50 cm s^{-1} are not uncommon (Harris et al. 1993). On examination of near bed (≈ 2 m above bottom) current speeds for sixteen fish farm sites in Scottish sea lochs (minimum 15 day record length), maximum hourly averages ranged between 5 and 26 cm s^{-1}. Diver observations, preliminary observations with a transmissometer (McKee unpublished data) and field trials of fish farm medicines (Scottish Environmental Protection Agency 1999) in these lochs, indicate that resuspension is a regular occurrence. Using a critical resuspension speed at the higher end of the reported range (e.g., 50 cm s^{-1}) would result in very few resuspension events taking place for these sites. Additional observational evidence for resuspension beginning at low shear stresses is given by Lund-Hansen et al. (1997) who observe an increase in light attenuation with a transmissometer at a bed shear stress of 0.015 N m^{-2} (≈ 9 cm s^{-1}) for several coastal sites. Experimental evidence given by de Jonge and Van de Bergs (1987) shows resuspension starting at 10 cm s^{-1} for a mixture of mud, sand and benthic diatoms in the Ems estuary, Netherlands. Burt and Turner (1983) also measured a critical resuspension speed of 15 cm s^{-1} for sewage sludge deposited on a sand rippled bed and numerous resuspension models have also been validated for low resuspension thresholds (Sanford et al. 1991; Southern Californian Coastal Waters Research Project [SCCWRP] 1992; Cromey et al. 1998). In these models, use of a low erosion threshold results in numerous resuspension events coupled with a low erodibility constant. The erodibility constant used by Sanford et al. (1991) ($M = 1.4 \times 10^{-6}$ kg m^{-2} s^{-1}) is much lower than values used by researchers who use high critical resuspension speeds (vr = 50 cm s^{-1}, $M = 3.0 \times 10^{-5}$ kg m^{-2} s^{-1}; Harris et al. [1993]). In this study, we test the validity of using a low critical resuspension speed and erodibility constant, thus generating frequent relatively small resuspension events.

The amount of material available for resuspension on the bed will also determine the magnitude of resuspension events, as consolidation of material will limit the amount of material which can be resuspended. Generally, consolidation is modelled either as some function of the amount of resuspendable material on the bed (Futawatari and Kusuda 1993), or probabilistically, where the probability of consolidation of a particle approaches unity as the time spent on the bed is increased (Sanford 1992). Resuspension models generally include a critical deposition speed (vd) where deposition occurs below this threshold. The range of critical deposition speeds reported in the literature is also wide ranging from 4.5 cm s^{-1} for sewage solids (SCCWRP 1992) to greater than 20 cm s^{-1} for estuarine models (Harris et al. 1993). Critical deposition speeds tend to receive less attention in both modelling and observations than critical resuspension speeds, and some doubts have been expressed on the need for a critical deposition speed at all when modelling cohesive sediments (Sanford and Halka 1993).

Salmonid fish farms can be studied as point sources of particulate material, discharging waste food and faeces of various settling characteristics and amounts. Our primary model is used for predicting the accumulation of particulate material (waste food and faeces) from these farms and has been validated for initial deposition of material from surface to sea bed. Little research has been undertaken on quantification of resuspension rates from areas surrounding fish farms and validation of the resuspension component of the primary model is required. For the sixteen fish farm sites studied, thirteen had hourly averaged current speeds which exceeded measured critical resuspension speeds for particulate material of 9 cm s^{-1} (SCCWRP 1992) and 15 cm s^{-1} (Burt and Turner 1983). Modelling of accumulation rates of discharged material at these sites will be greatly improved by including a resuspension component generally lacking in current models applied to this problem (Gowen et al. 1989; Silvert 1992; Hevia et al. 1996; Gillibrand and Turrell 1997). The aims of this study were to quantify the resuspension of a point source of tracer representing fish farm wastes in a typical sea loch environment and use these results to validate a resuspension model and

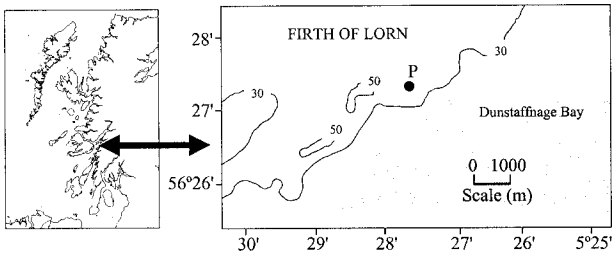

Fig. 1. Study area in the Firth of Lorn, Scotland, UK with chart datum bathymetry in metres. Tracer release point and current meter mooring (P ●) at 56°27.3′N, 5°27.6′W.

obtain a set of model parameters for future testing of a primary model of aquaculture discharges.

Study Location

The tracer experiment was situated in the Firth of Lorn, a fjordic sea loch system on the west coast of Scotland (Fig. 1). Water depth in the study area varied between 30–40 m, and the sea bed was a silty mud. Pre-survey measurements taken previously (Aanderaa RCM7, Bergen, Norway; 10 min interval, 26 day deployment), showed near-bed (z = 2 m) current speeds had a mean and maximum speed of 4.9 and 23 cm s^{-1} with a residual speed and direction of 2.9 cm s^{-1} and 069° respectively.

Materials and Methods

Ultraviolet fluorescent tracer particles (Parchvale Technical Products, Banbury, UK) with similar physical properties to the average properties of fish farm wastes were required (ϕ = 2–6 mm, settling velocity ≈ 3.4 cm s^{-1}; Chen et al. 1999; Cromey et al. 1999). The use of this specific tracer for determining dispersion of discharged solids from a variety of sources is well tested (Marsh 1995). To achieve these properties, a calibration curve of settling velocity versus specific gravity was required using particles with a range of specific gravities. To determine settling velocity of tracer particles, a perspex settling column (l = 3.1 m, ϕ = 0.1 m) containing unfiltered sea water from the laboratory flow through system was used. After treatment with surfactant, particles were introduced sub-surface and allowed to settle in the column. After cessation of acceleration approximately one metre from the surface, settling rates were then determined over the next metre. From the calibration curve established, a specific gravity of 1.127 was selected.

215 kg of raw tracer containing an undesired wide size range of particles was separated into twenty equal batches and sieved onto a 2 mm mesh. The residue tracer (particle ϕ = 2–6 mm) was then mixed into a slurry containing seawater and surfactant (Decon 90) to facilitate sub-surface

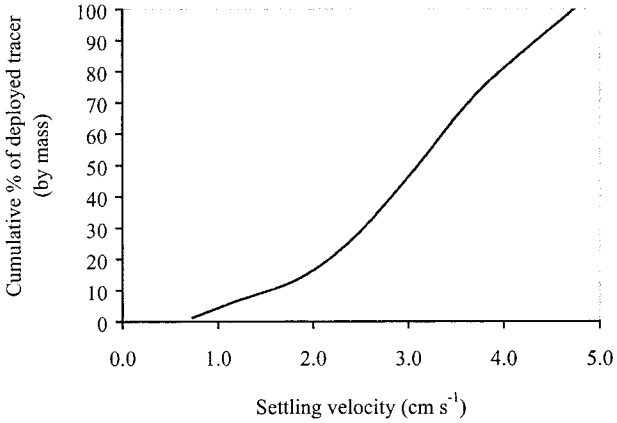

Fig. 2. Settling velocity distribution of deployed tracer shown as cumulative percentage mass (n = 191 particles).

deployment of the tracer and placed in a 100 l drum. A 500 ml subsample was removed from each batch before and after treatment with surfactant. To facilitate calculations of mass of tracer deployed, washings from the raw tracer that passed through a 2 mm sieve were collected in a 0.5 mm sieve and weighed. The washings were mixed thoroughly in a 100 l drum and a sub-sample was weighed before and after drying at 50°C for ten days. The total mass of washings was then determined from the mass of the sub-sample and subtracted from the raw tracer mass (215 kg) to determine the total mass of deployed tracer (155 kg). Sub-samples of deployed tracer were used in settling velocity experiments to verify characteristics and for use as model input (Fig. 2).

The discharge of tracer started on April 27, 1999, at 14:00 GMT for approximately 2 hours. A pump was used to discharge the tracer to the seabed via a 30 m long hose, weighted and positioned vertically down ca. 3 m from the sea bed. A prior test deployment monitored by underwater video equipment showed that this method of discharge prevented injection of the tracer into the sediment and/or rebounding of the tracer plume off the sediment into the water column. Day 0 sampling was undertaken to check that no tracer was present before deployment. The actual distribution of the tracer on the same day of the deployment was unknown, as any sampling of the area after deployment would interfere with the initial deposition of the tracer. Thus, to prevent any such interference, the first sampling event was on day 3. The nature of fish farm discharges and the cage groups that create them gives rise to ''pile'' characteristics (Silvert and Sowles 1996). Our own sediment trap observations demonstrate very large deposition gradients over small spatial scales ~25–50 m (Cromey

et al. 1999) giving further value to this deployment method.

The model was run pre-deployment of tracer with test parameters to predict tracer concentrations and assist in definition of the sampling grid area and extent. A radial sampling grid was established from the center of the tracer deployment (56°27.260′N, 5°27.580′W), with several stations at the center of release. Stations were then positioned concentrically at radii of 25, 50, 100, 150, 200, 400, 700 and 1,000 m from the source, on transects 30° apart (30°, 60°, 90° etc.), and fixed by differential GPS. Quantitative sea bed samples were taken at these stations using a van Veen grab (0.1 m^2) on days 0 (pre-deployment), 3, 10, 17 and 30. This equates to 39, 34, 29 and 33 grab samples for the post deployment days respectively. The main sampling effort was devoted to the 60° transect, as previous current meter data had established a residual current along the direction of this transect. With the exception of this transect, all transects were sampled to a minimum of 150 m and were not completely sampled beyond this if 2 consecutive stations revealed no tracer in the grab sample; stations were sampled further along transects if tracer was found at inner stations. On day 30, two additional transects at 45° and 75° were added and sampling along the 60° transect increased. Sampling along these transects was undertaken at 400, 550, 700, 850 and 1,000 m from the source to confirm by mass balance that the tracer had been completely dispersed. The grab samples were subsampled by cores (ϕ = 5.7 cm), which were in turn sliced into 2 cm sections, to establish the vertical distribution of tracer in the sediment. Whole grab and core subsamples were sieved onto 2 mm mesh on deck and sieve residues were returned to the laboratory for enumeration and gravimetric analysis. Using a long wavelength UV lamp, individual particles were picked from each sieved sample, washed thoroughly and then dried overnight in an oven at 50°C. Samples were then weighed to determine mass per 0.1 m^2. Where large numbers of particles were in the sample, after counting the particles, a sub-sample (size $\geq$ 25% of total numbers) was taken for subsequent washing, drying and weighing. The mass of the whole sample was then determined from the mass of this sub-sample.

An electromagnetic current meter (Interocean S4, San Diego, California) was deployed 2 m above the bed at the release point for the duration of the experiment. Instrument failure, however forced meter redeployment after the experiment had ceased resulting in two current records being available for the study, a pre and post-release data set (length $>$ 2 spring-neap cycles). Two approaches were used to obtain modelled and observed (phase-aligned) current data. A harmonic analysis was performed thus enabling currents to be predicted at the time of release. In the analysis, a standard set of 32 major and 8 related tidal constituents were used including mean and long period constituents. The longest period constituents (i.e., z_o, Mm, Msf) had periods less than the length of the current record used in the analysis. The phase of the Spring-Neap envelope was used to align the previous observations with the phase of the envelope for the day of release. Analyses were also undertaken to test the sensitivity of the model using modelled and observed (phase aligned) currents detailed in the discussion.

Site bathymetry and sea bed characteristics were determined by acoustic ground discrimination, using the RoxAnn (Marine Micro Systems, Aberdeen UK) system, utilising a 200 kHz transponder. Bathymetry was adjusted for height of tide at the time of measurement to obtain lowest astronomical tide (LAT) referenced depth.

The Model

The bathymetry measured was used to generate a rectangular model grid containing depth (LAT referenced), sampling station positions and position of the release point. In the model, mean tidal height for Oban was added to the depth and no further adjustment made for tidal elevation changes. The small height of the release point above the bed and the modelling of near bed particle transport rendered the modelling of tidal elevation change unnecessary. The model grid had a total size of 1.8 by 1.4 km with grid cell resolution of 10 m. The model grid size and resolution was chosen to incorporate the sampling station 1000 m from the release point and allow sufficiently fine resolution in the inner sampling grid surrounding the release point. The accuracy of the grid generation algorithm for reproducing observed bathymetry has been tested at a site with similar bathymetry and found to be acceptable (R^2 = 0.96, n = 424, α = 0.05 2 tailed, y = 0.98 x where y is the predicted and x is the observed depth). Land cells defined in the model grid cause a particle to be reflected back to its position in the previous time step. The release point was located in the model grid at position (0, 0). Discharged particles will sink or float through the water column characterised by its depth, viscosity, density, mean current regime and turbulence. The particle tracking model deals with the three dimensional trajectory of the particle from the point of discharge to the sea bed. This is modelled as an ensemble of individual particle trajectories by a simulation of the bulk properties of the particle ensemble (Mead 1991; Mead and Rodger 1991). In modelling the hori-

zontal trajectory of a particle it is convenient to consider the current as a sum of two parts: a slowly varying advective component relating to tidal or wind forcing plus a more rapidly varying component relating to turbulence with a mean value of zero. Random walk has been implemented into the model as a representation of turbulence (Allen 1982). The magnitude of particle trajectory in this model is dependent on the size and direction of the random excursion and the time in the turbulent field defined by its settling velocity:

$$rw_{step(x)} = rw_{dir}\sqrt{2k\delta t} \quad (1)$$

where $rw_{step(x)}$ is the step length in the x direction (m), rw_{dir} is the step direction + or − (determined from a random number generator), k is a dispersion coefficient ($m^2\ s^{-1}$) and δt is the time in the turbulent field (s). For a particle position defined as $P_{(x,y,t)}$ and current velocity components u and v for a height above the bed (z), then horizontal transport for each time step of length t can be defined as

$$P_{(x,y,t+1)} = P_{(x,y,t)} + u_{(z,t+1)}\delta t + rw_{step(x)} + v_{(z,t+1)}\delta t + rw_{step(y)}. \quad (2)$$

In the vertical direction given a settling velocity of vs, the vertical step is

$$P_{(z,t+1)} = P_{(z,t)} + vs\delta t + rw_{step(z)}. \quad (3)$$

Current direction data were adjusted for magnetic variation and hourly averages were calculated from velocity u and v components to describe the advective component of the transport. The trajectory of a particle was calculated every 60 seconds in the model (δt) which is appropriate for the high settling velocities of the waste materials modelled. The total mass of particles released in the model was 155 kg over 2 hours similar to the field discharge and released from a point source 3 m above the sea bed in a depth of 31.5 m in the model grid. Model particles were assigned a settling velocity distribution similar to the tracer and a total of 1.4×10^4 particles were released from the point source. Increasing the number of particles further increased computational time but gave no change in the bed distribution of the particles during initial deposition.

A resuspension function which takes account of the current velocity ($U_{(z)}$) at some reference height above the bed (z) and a critical current velocity for resuspension (vr) is given by Uncles et al. (1985):

$$M_e = M\left(\left(\frac{U_{(z)}}{vr}\right)^2 - 1\right) \quad (4)$$

where M_e is the rate of erosion ($kg\ m^{-2}\ s^{-1}$) and M is an erodibility constant ($kg\ m^{-2}\ s^{-1}$). The model uses a variation of this formula substituting current velocity for bed shear stress where the erosion rate is a function of the erodibility constant and the amount by which the critical bed shear stress (τ_{ce}) is exceeded by the bed shear stress (τ_b)

$$M_e = M\left(\frac{\tau_b}{\tau_{ce}} - 1\right). \quad (5)$$

To allow calculation of the bed shear stress from the measured current velocity near the bed, bed shear velocity U_* ($m\ s^{-1}$) is used in the following relationship (Bowden 1983):

$$\tau_b = \rho U_*^2 \quad (6)$$

where ρ is the density of seawater ($\approx$ 1,025 kg m^{-3}). Tidal stratification and variation in ρ in Eq. (6) has been shown to cause a variation in shear stress even when currents are equal (Lewis and Lewis 1987). Because the small variations in density at the sea bed are unlikely to be significant at the study site, density was taken as constant. There is both theoretical and experimental evidence that a logarithmic profile exists in the boundary layer (McLellan 1965; Neumann and Pierson 1966; Bowden 1983) which can be used to calculate U_*. Hethershaw (1988) reports a range of hydraulic bottom roughness lengths (z_o) of $2–7 \times 10^{-4}$ m. Using a z_o of 2×10^{-4} m for a muddy bottom (Soulsby 1983), data from the instrument which was deployed close to the bed (i.e., z = 2 m) can be used to define a logarithmic profile from this point to the bed by the following relationship (Dyer 1979):

$$U_* = \frac{\kappa U_{(z)}}{\ln(z/z_o)} \quad (7)$$

where κ is the von Kàrmàn constant. Our model uses the shear stress erosion formula in Eq. (5), but U_* has been substituted into Eq. (5) and validated for the Gironde estuary by Teisson (1991) and Puls and Sündermann (1990).

Deposition occurs when the bed shear stress is less than the critical shear stress for deposition (τ_{cd}) as given by:

$$M_d = vs \cdot pe\left(1 - \frac{\tau_b}{\tau_{cd}}\right) \quad (8)$$

where M_d is the rate of deposition ($kg\ m^{-2}\ s^{-1}$), vs is particle settling velocity ($m\ s^{-1}$) and pe is particle concentration ($kg\ m^{-3}$). Both of these models assume that $\tau_{cd} < \tau_{ce}$ so that deposition and erosion processes are separate and that M_d and M_e are zero for the conditions $\tau_b \geq \tau_{cd}$ and $\tau_b \leq \tau_{ce}$ respectively (Krone 1962; Parthenaides 1965; Odd and Owen

1972). When particles are resuspended for the condition $\tau_b > \tau_{ce}$, they are transported at the same velocity as the measured near bed current velocity until deposition occurs when $\tau_b < \tau_{cd}$. The field results showed minimal downward transport of tracer in the sediments. In the model, the incorporation of tracer material was set to zero so that all tracer remained available for resuspension.

Model parameters were kept constant for individual runs but between runs parameters were varied within reasonable bounds to determine the best agreement between observed and modelled tracer concentrations. Keeping close to literature values, τ_{ce} was varied between 0.009 N m^{-2} and 0.045 N m^{-2} (vr $\approx$ 7 and 15 cm s^{-1} respectively using Eqs. 6 and 7; $\rho \approx 1025$ kg m^{-3}, z = 2 m, $z_o = 2 \times 10^{-4}$ m, $\kappa = 0.4$) and τ_{cd} kept close to 0.004 N m^{-2} (vd $\approx$ 4.5 cm s^{-1}). When comparing these critical resuspension speeds with other authors' data, the exact height of the instrument above the bed (z) is relatively unimportant above a critical height. Using these parameters and varying z in Eq. (7) greater than 0.8 m, results in a change in U(z) which is within instrument accuracy (manufacturers' specification $\pm$ 1 cm s^{-1}). The erodibility constant M cannot easily be quantified from the literature so this value was the main parameter varied between model runs to achieve best agreement with field data.

Comparison of Observed and Modelled Tracer Concentration

In order to compare observed and modelled concentrations some scheme must be devised which allows comparison on a spatial and temporal scale. An attempt was made with several contouring algorithms to contour observed data for each sampling event and produce a visual plot of the survey area for comparative purposes. No algorithm was found which suitably contoured the observed data without producing large spatial anomalies that were artefacts of the contouring. In addition, mass budgets calculated from the contoured observed data gave a total release of 255 kg of tracer on day 3, when only 155 kg was released. Between sampling events, sampling stations were not always positioned in exactly the same place due to practical considerations of vessel positioning and varying weather conditions. As this prevented a time series of observed concentration being generated for each station, a scheme was used which defined sectors at various distances from the release point. The survey area was separated into 4 direction sectors of 90° each with sector A centerd around the 060° transect shown in Fig. 3. Sector A is representative of an area of 015° to 105° true, sector B 105° to 195°, sector C 195° to 285° and sector D 285° to 015°. Each sector is further divided into four areas at varying distances from the release point with sector A50 representing the area 25 to 50 m from the release point; A100, 50 to 100 m; A200, 100 to 200 m and A200+, 200 to 1,000 m. A circle of 25 m radius around the release point encloses the inner circle (R). No measurements were made in sectors B200+ or D200+ as the tracer was not found beyond sectors B50 and D50. Total amounts of measured tracer in each sector were calculated by using averaged concentrations (g m^{-2}) for all sampling stations in a sector and multiplying by sector area. A similar scheme was used for modelled concentrations and comparisons made between observed and modelled sector totals only where sectors had been sampled. Using this scheme for the four sampling events with 15 sectors each, a total of 90% of the sectors were sampled on all sampling days. This scheme has several advantages as it is designed to suit the radial sampling grid strategy with frequent sampling in each sector. By this method, a mass budget for day 3 gave a total of 137 kg of tracer measured in the grid area where 155 kg was released on day 0. Observed mass budgets throughout the study period have been tabulated and are compared with modelled data.

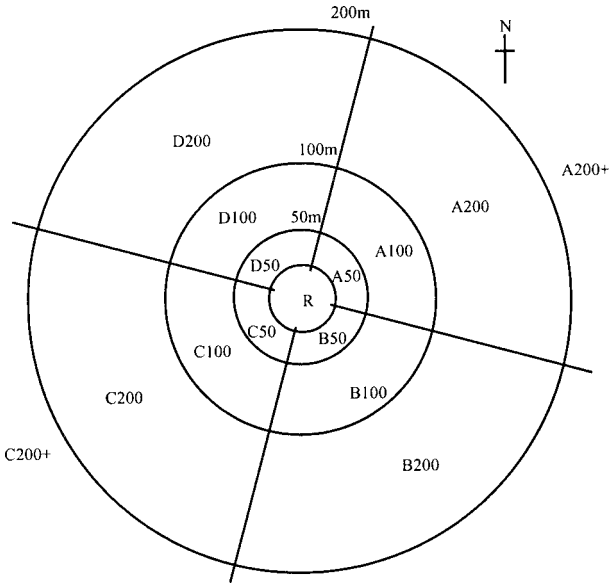

Fig. 3. A schematic diagram showing the division of the study area into different sectors used for comparisons of modelled and observed data.

Results

Field Techniques

Water depth at the release point was 31 m with a generally flat sea bed in the near vicinity (Fig.

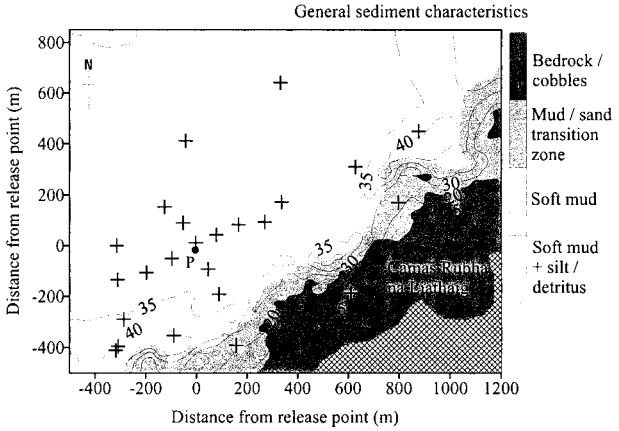

Fig. 4. Bathymetry for the study area showing lowest astronomical tide referenced depth contours and general sediment characterisitcs interpolated using RoxAnn™ and ground truthing data (denoted by +). Tracer release point (P●) is at position (0, 0).

4). Sloping bathymetry towards the shore reduced to a depth of less than 30 m at approximately 300 m south east of the release point. Areas deeper than 40 m were measured 800 m ENE and 400 m SSW from the release point. Sediment samples collected in the survey area at each sampling station were generally sandy mud and homogenous in the vicinity of the release point verifying RoxAnn data. Areas closer to the shore in depths less than 30 m showed a graduation from sandy mud to bedrock.

The positions of the sampling stations for all sampling events are shown in Fig. 5. The tidal components determined by harmonic analysis accounted for approximately 70% of the variance within the observed currents, demonstrating the tidal nature of the site. The tides were dominated by the semi-diurnal constituents with the largest constituent being M2 at 5.5 cm s^{-1}. Figure 6 shows the phase aligned and modelled currents for the 30 days following release of the tracer.

Comparison of Observed and Modelled Tracer Concentration

Core subsamples revealed no tracer penetration below 2 cm at any station and so all results described are for tracer measured in this surface sediment layer. Table 1 shows the change in observed and modelled concentrations in each sector with time. For day 3, the highest observed concentrations of tracer are in the inner circle (R) and contribute to a significant amount of the total released. Tracer was found in sectors in the direction of the residual current along the 60° transect (sectors A100, A200) and the 240° transect (C100). No tracer was found beyond sector A200 or in any other sectors for this sampling event. The change in

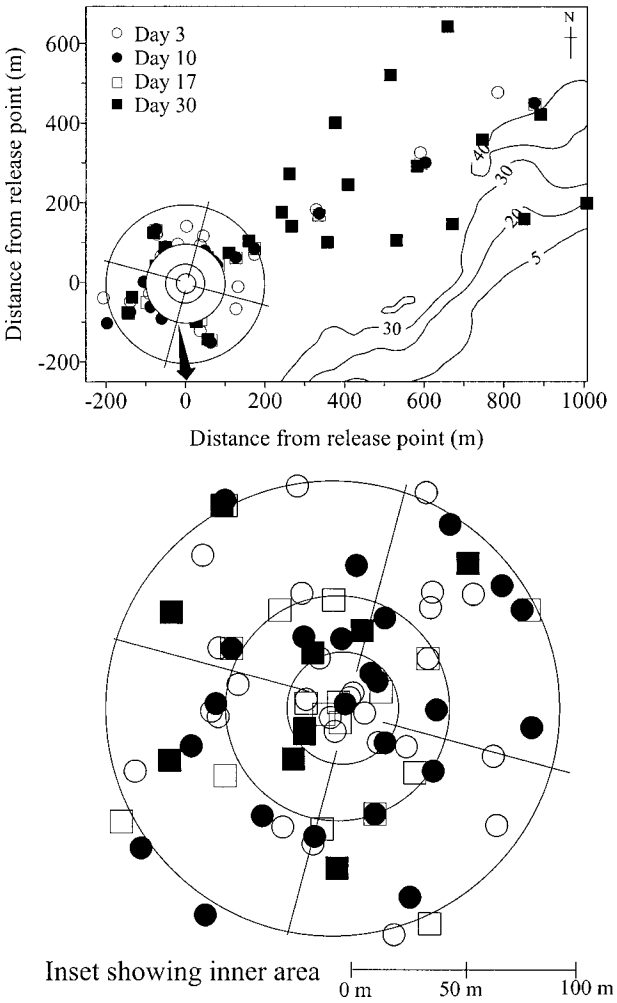

Fig. 5. The study area showing station positions for each sampling event (○ denotes a station sampled at Day 3, ● on Day 10, □ on day 17 and ■ on day 30).

the observed tracer concentration between day 3 and 10 was significant with resuspension of material causing the concentration for the whole grid to be reduced from 88% of the total released to 39%. Although the bulk of the tracer was distributed within the central area for day 10, 6.4% of the total tracer released was found up to 200 m from the release point in the direction of the residual current (A100, A200). Between day 10 and 17, resuspension of material was lower than the previous seven day period causing a reduction for the whole grid from 39% to 5% of total released (Table 1). Complete erosion of material had taken place around the release point (inner circle R) and tracer was again found in sectors A100 and A200 (4.9% of total released). Complete resuspension of the remaining tracer took place between day 17

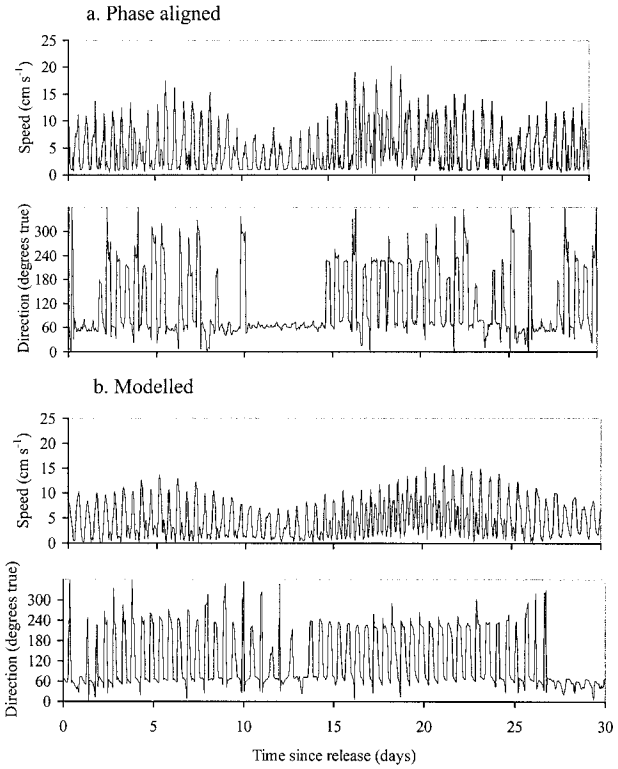

Fig. 6. Observed (phase aligned) (a) and modelled (b) near-bed current speed and direction at the release point.

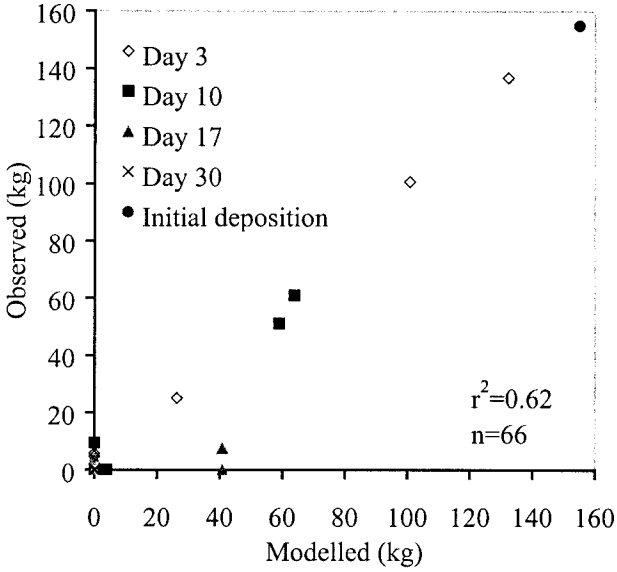

Fig. 7. Comparisons between observed and modelled concentration of tracer in all sectors for different sampling events (r^2 is product moment correlation coefficient for log transformed (x + 1) data). For the initial deposition mass budget comparison (●), all of the 155 kg of tracer released is assumed to deposit in the sampling area and was not included in any statistical calculations.

and 30 with very low concentrations of tracer being found up to 200 m from the release point.

Optimum agreement between model and field observations were obtained for critical shear stress values of resuspension (Eq. 5) and deposition (Eq. 8) of 0.0179 and 0.004 N m^{-2} respectively. Using Eqs. 6 and 7, these shear stress values correspond approximately to near bed current speeds of 9.5 and 4.5 cm s^{-1}. With these parameters, an erodibility constant M (Eq. 5) of 7×10^{-7} kg m^{-2} s^{-1} gave the best agreement with observations. The model results described are based on these resuspension model parameters.

Initial deposition of the modelled tracer in Table 1 shows the majority of the modelled tracer initally depositing near the release point with 72% of total tracer released in the center of the grid (inner circle R). Initial deposition of the tracer was also found in sectors A50 and A100 in the direction of the residual current. Comparisons between observed and modelled concentrations of tracer close to the release point were generally good where concentrations were high for the whole of the experiment except day 17. Movement of tracer in the direction of the residual current was also shown in the model and some deposition of tracer in the model was found 850 m from the source in the direction of the residual current. This was not detected despite sampling of this area throughout the study.

Direct comparisons of modelled and observed concentrations are shown in Fig. 7. Model performance is good at high concentrations of tracer

TABLE 1. Comparisons between observation and model output for the main area surrounding the release point (inner circle R), A sectors, and all other sectors as a percentage of the 155 kg of tracer released (— denotes not sampled).

	Percentage of Total Released							
	Inner Circle (R)		A Sectors		All Other Sectors		Total	
Time (d)	Obs.	Mod.	Obs.	Mod.	Obs.	Mod.	Obs.	Mod.
Initial deposition	—	71.6	—	25.8	—	2.5	—	100.0
3	64.9	65.0	22.8	19.0	<1	1.3	88.3	85.3
10	32.9	38.0	6.4	3.1	0	0	39.3	41.2
17	0	26.4	4.9	0	0	0	4.9	26.4
30	0	2.0	0	<1	0	0	0	2.0

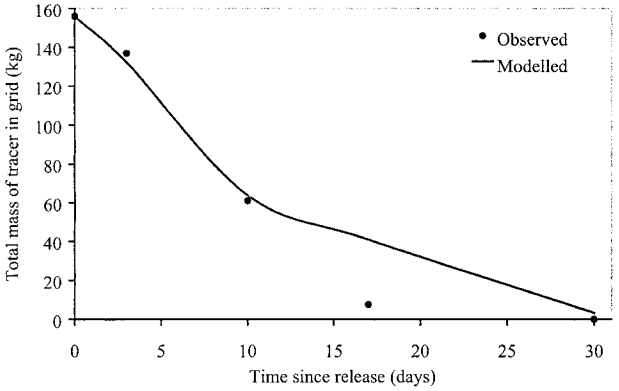

Fig. 8. The total change in observed tracer mass with time and model predictions.

near the release point, with performance being reduced as concentrations are reduced. The changes in observed and modelled total mass budgets are shown in Fig. 8 with all sampling events being fitted with the exception of day 17.

Discussion

Applicability of the Model

This study improves the predictive capability of our primary model (DEPOMOD), which is regularly used for assessment of fish farm discharges by U.K. regulators and the industry alike. Dudley et al. (2000) have recognised the importance of resuspension in fish farm modelling and have measured resuspension for model validation in the U.S. Application of fish farm models in the U.K. have until now, been mainly undertaken without resuspension included. Modelling the redistribution of particulate pollutants from fish farms cannot be undertaken adequately without a resuspension component for all but the most quiescent of sites. Carbon (Ackefors and Enell 1994; Holmer and Kristensen 1994), chemotherapeutants (Davies et al. 1996; Black et al. 1997) and heavy metals (Uotila 1991; Miller 1998; Morrisey et al. 2000) may all be potentially redistributed away from fish farms by resuspension. Other factors such as the oxygen demand (Hansen et al. 1991) and fluctuation in oxygen supply from near bed currents (Findlay and Watling 1997) may be just as important in assessing impacts. Resuspension may have relevance for enhanced redistribution of wastes assisting benthic recovery of sediments during farm fallow periods. Resuspension is likely to be equally important for redistribution of pollutants associated with other types of particulate discharges such as sewage (Cromey et al. 1998), distillery wastes (Nickell and Anderson 1997), trace metals from spoil grounds (Rodger et al. 1992) and drill cuttings (Delvigne 1996). This study also gives some evidence for the behaviour, and modelling, of piles of recently deposited material (Wolanski and Gibbs 1992; Moon et al. 1994; Michels and Healy 1999).

In the present study, resuspension of a particulate tracer from a point source over 30 days has been measured and used to validate a Lagrangian model. For all sampling events, the model predicted within ± 8% of total tracer released for an area surrounding the release point. Total mass budgets for the grid area were predicted within ± 7% of total released and for the A sectors within ± 3%. The main source of differences between the model predictions and observations are for day 17, otherwise the model predicts observations adequately. One or a combination of the following may account for these differences and these are discussed below: limitations in the modelling of some process; sampling strategy and sector scheme or model input data.

Limitations of the Model

The main processes of the model, erosion–transport–deposition–consolidation, are taken from established models reported in the literature. These processes have rarely been validated for fish farm wastes as achieved in the present study. Consolidation per se, was not modelled as field results showed that vertical movement of tracer in the sediments was minimal and so this part of the model was not tested. Flocculation processes were not modelled as the tendency for these large diameter tracer particles ($\phi \approx 2$–6 mm) to flocculate causing a significant change in settling velocity is unlikely. In addition, the model overestimated tracer concentrations at day 17 and so the use of a flocculation model, which would increase deposition, is unlikely to improve model performance. Spatial variation in the currents was not modelled across the grid area and this source of error will become more significant at increasing distance from the release point. At distances up to 200 m there is little change in the bathymetry to suggest that spatial variation in the current would be a significant source of error at the study site.

Sampling Strategy and Sector Scheme

Dividing areas around the release point into sectors with an inner circle R, gave sensible mass budgets which could not be obtained by contouring methods. Sectors were well sampled with a total of 90% of all sectors being sampled for all sampling events. Table 2 shows the number of grabs taken in the inner circle and A sectors compared along with the predicted number of particles per grab area. Grab sampling was the most frequent in the inner circle where tracer concentrations were high with a general increase in grab sampling per sector

TABLE 2. The modeled number of particles (P_{mod}) per grab (0.1 m^2) compared with the actual numbers of grabs taken per sampling event for the inner circle and the A sectors.

Sampling Event	Inner Circle (R)	A50	A100	A200	A200+[1]
Day 3					
P_{mod} per grab	547	143	0	0	2
Grabs taken in sector	8	1	3	4	3
Day 10					
P_{mod3} per grab	458	108	0	0	1
Grabs taken in sector	4	2	4	2	3
Day 17					
P_{mod} per grab	370	0	0	0	0
Grabs taken in sector	5	1	1	2	3
Day 30					
P_{mod} per grab	165	0	0	0	1
Grabs taken in sector	2	1	1	2	16

[1] The small area in sector A200+ in the model grid 850 m from the release point which contained deposited particles was sampled in the field as follows: 1 grab on days 3, 10, and 17; 2 on day 30. No tracer particles were detected.

between A50 and A200. Increased sampling took account of the sector area increase between A50 and A200 and the wider dispersion of the tracer at increasing distances from the point source. With regards to the day 17 event, 5 grabs were taken in the inner circle and no tracer found. The model predicted large quantities of tracer and so the model and/or input data are likely to be the cause of error for the inner circle. From a sampling viewpoint, total mass budgets on day 17 for the observed tracer may have been underestimated due to low sampling in the A50 and A100 sectors. Although sectors A200+ and C200+ represent a large sector area (Figs. 3 and 5), no tracer was found in these sectors and so the limitations of the sector scheme for these large area sectors can be safely ignored.

To test the significance of possible under-sampling, an assessment is required on the effect on the total mass budget of finding one extra particle in a grab for one of the large sector areas. For the largest sectors A200+ and C200+, no particles were found and so the next largest sector A200 can be used for this assessment. Four, 2, 2 and 2 grabs were taken in sector A200 for days 3, 10, 17 and 30 respectively (Fig. 5). Finding one extra particle with a mass of 17.4 mg (mean mass of particles sampled) in one grab for the sector area of 23,562 m^2, equates to an additional mass of 1.0, 2.1, 2.1 and 2.1 kg for days 3, 10, 17 and 30 respectively. In terms of the total mass balance (Table 1), this would increase mass budgets for each sampling event to 89.3, 41.4, 7.0 and 2.1 kg thus improving model performance. i.e., performance would be improved from ± 7% to ± 5.9% of total tracer released. It is felt that under-sampling would not reduce the agreement between observation and predictions. On the contrary, if further sampling resulted in finding additional particles then agreement would have been improved.

Accuracy of Model Input Data

The use of observed (phase aligned) and modelled current instead of true current data measured during the study did not seriously hinder validation of the model. Small differences in parameters were obtained for the same level of performance using the observed and modelled data which further verifies the tidal nature of the site. In both data sets, currents between day 10 and 17 were lower than previous periods as a neap tide occurred on day 12 resulting in fewer resuspension events. During this period of low current, the lack of true current measurements cannot be completely ruled out as a possible cause of error. From daily observations taken at Dunstaffnage Marine Laboratory meteorological station, the weather during this period was generally settled, thus a wind driven event is unlikely to be the cause of significant resuspension during this period.

Model Performance at Low Tracer Concentrations

Model performance improved as tracer concentrations increased closer to the release point. For concentrations less than 1 g m^{-2} (≈ 5 particles per grab) between 50 and 200 m from the release point, model predictions were less accurate. The reason for reduced performance is likely to be due to the resuspension model processes and the difficulty with the model being unable to transport particles short distances. For the majority of fish farm sites studied, the main area of initial deposition is typically within a hundred metres of the cage group due to the high settling velocities and the low dispersive nature of the areas where many of the farms are sited. The nature of the model made predicting redeposition close to the release point difficult as transport of resuspended particles resulted in net loss of material from the area. For example, resuspension of particles occuring at an hourly averaged speed of 15 cm s^{-1} would result in these particles being resuspended and transported a distance of 540 m. Redeposition of these particles would then only occur if the next time step resulted in current speed being less than the deposition speed (≈ 4.5 cm s^{-1}). Using a shorter time step of ten minutes could potentially improve the predictions in this 50–200 m zone as a smaller transport step of 90 m would result from a current speed of 15 cm s^{-1}, but a low current speed in the subsequent time step would still be required to result in

TABLE 3. A table showing model performance for the best fit of model parameters and sensitivity analysis of resuspension model parameters. The best fit was obtained using phase aligned currents and sensitivity analysis was undertaken using these currents. The best fit using modeled currents is also shown.

Model Run	Critical Resuspension Speed (vr) cm s^{-1}	Critical Deposition Speed (vd) cm s^{-1}	Erodibility Constant (M) kg m^{-2} s^{-1}	Model Performance[1]		
				α	r^2	t_s
Best fit	9.5	4.5	7.0×10^{-7}	13,439	0.62	10.3
Vr − 25%	7.1	4.5	7.0×10^{-7}	19,378	0.63	10.5
Vr + 25%	11.9	4.5	7.0×10^{-7}	11,274	0.43	6.9
Vd − 25%	9.5	3.4	7.0×10^{-7}	13,439	0.62	10.3
Vd + 25%	9.5	5.6	7.0×10^{-7}	13,439	0.62	10.3
M (threefold decrease)	9.5	4.5	2.3×10^{-7}	11,261	0.45	7.2
M (threefold increase)	9.5	4.5	21.0×10^{-7}	554,607	0.38	6.3
Modeled currents[2]	9.0	4.5	14.0×10^{-7}	13,457	0.64	10.6
Modeled currents[3]	8.2	4.5	6.4×10^{-7}	13,491	0.58	9.3

[1] α is a measure of goodness of fit $\Sigma\ (O - E)^2/E$ for observed and expected (modeled) tracer mass budgets for each sector and total grid area for each sampling event ($n = 66$). Parameters were varied to minimise α. In calculation of α, 0.013 kg, which was the smallest detected mass, was added to O and E to allow inclusion of zero values of E in the calculation. Product moment correlation coefficient denoted by r^2 is for log transformed $(x + 1)$ observed and modeled budgets and t_s is t-test statistic for correlation coefficient $r\sqrt{(n-2)}/\sqrt{(1-r^2)}$. t_{crit}(2 tailed, $\alpha = 0.01$, d.f. $= n - 2$) is 265.

[2] Best fit obtained for modeled currents using resuspension model parameters reported by Sanford et al. (1991).

[3] Using a similar erodibility constant M to the best fit with observed current, a lowering of vr was required with modeled currents to obtain a satisfactory fit.

deposition. Despite this, testing of the model with a time step of 10 minutes did not improve model perfomance.

The use of a range of erosion thresholds dependent on particle size or tidal action (Clarke and Elliot 1998) may improve model performance in the 50–200 m zone. A lower threshold either due to a smaller particle size or scouring of the bed during a dynamic period, would result in resuspension occurring at lower current speeds with shorter transport steps. Spatial variation of shear stress across the bed (Mehta 1984) may be a cause of model spatial errors. At quiescent sites where the critical threshold is only just exceeded, shorter transport steps may be produced in the model. For this particular study redeposition in the model is found at distances of 850 m from the source and these transient depocenters in the model appear to be the minimum distance that redeposition is occurring.

Sensitivity Analyses

The best fit of field data using Pearson's statistic was obtained using phase aligned currents (vr $\approx$ 9.5 cm s^{-1}, vd $\approx$ 4.5 cm s^{-1}, M $= 7.0 \times 10^{-7}$ kg m^{-2} s^{-1}). Both decreases in critical resuspension speed and increases in erodibility constants (i.e., increasing frequency and intensity of resuspension events) were found to be the most sensitive parameters in the model. Increases in vr and decreases in M showed less sensitivity in the model. Although the sensitivity of the parameter vr highlights the need to measure currents accurately, the differences in current between the observed and modelled currents only slightly affected the setting of vr (i.e., vr $\approx$ 9.5 cm s^{-1} for observed, vr $\approx$ 9.0 cm s^{-1} for modelled). The main reason for this difference is probably caused by the occasional peaks in the observed current, which generate larger than average resuspension events (Fig. 6). Lesht (1979) related turbidity to the statistical frequency of bottom shear stress in a way that implies a few high stress events are responsible for the bulk of resuspension events. Thorne et al. (1989) describe evidence for bursting events, resuspension events driven by instantaneous increases in near bed turbulent velocity fluctuations. Using less noisy modelled current in this model has shown that a lower vr is required for the same model performance as peaks in the observed data were the main drivers of resuspension. Using modelled current to drive a resuspension model at a mainly wind driven site is likely to compound these differences. Predictions were insensitive to varying vd, suggesting that erosion and transport are the main processes in the model. The use of a low vr and the lack of spatially varying current prevent prolonged deposition events or significant depocenters forming. Model parameters used by Sanford et al. (1991) to determine the influence of tidal resuspension on the erosion of recently dredged sediment deposits in Chesapeake Bay gave the best fit for modelled current in this study (Table 3). Although these researchers conclude that the critical erosion stress is at the low end of the reported range, our study also verifies that critical erosion thresholds of recently deposited material are much lower than thresholds typically used for modelling suspended sediment in coastal models.

Comparison of Resuspension Rates

It is useful to make some comparisons with reported resuspension rates for similar coastal environments. From our study, resuspension rates of tracer material during all resuspension events were between 8×10^{-4} and 9 g m^{-2} hr^{-1} with a mean and median of 1.8 and 1.3 g m^{-2} hr^{-1} respectively. At the release point where the amount of resuspendable tracer in the model was only limiting near the end of the study period and field observations were best predicted, approximately 7 g m^{-2} d^{-1} were resuspended over the period of the study. Lund-Hansen et al. (1997) measured sediment resuspension of naturally occurring sediments from three Danish fjords, two of which were exposed, between 4 and 82 g m^{-2} d^{-1}. Roman and Tenore (1978) measured resuspension rates of natural material of 130 g m^{-2} d^{-1} in Buzzards Bay, Massachusetts and Hendricks (1987) measured a resuspension rate of 55 g m^{-2} d^{-1} near Californian sewage outfalls sited in 40–60 m depth. Fleming and Walker (1981) calculated a general figure of 0.5 g m^{-2} d^{-1} for resuspension of sediments in Loch Eil. Although this general figure of 7 g m^{-2} d^{-1} is at the lower end of these reported values, the time scale over which these values have been resolved will significantly influence the calculation (Nichols 1985).

Conclusions

This study describes the validation of a resuspension model using a particulate tracer with similar physical characteristics of fish farm wastes. The model generally predicted total mass budgets satisfactorily (± 7% of total tracer released), particularly where tracer concentrations were high near the release point.

While the compartmentalisation of resuspension processes in the model are simplistic (though well documented and validated), increasing the complexity of the model would result in additional parameters requiring quantification and testing in sensitivity analyses. This validated resuspension model is a significant advance on models currently applied to aquaculture discharges in the U.K. The target user community (regulatory authorities and aquaculture industry) required the model be designed so that it can be widely applied using data routinely collected for each fish farm discharge. The model does not require additional data collection which would restrict its use.

The parameters used in the model are at the lower end of reported values used in estuarine and coastal models. However, our parameters agree with those reported by researchers studying the tidal resuspension of sewage and recently dredged deposits. This suggests that for freshly deposited material which has a low erosion threshold, the frequency of resuspension and deposition events is high.

Acknowledgments

This work was carried out as part of the NERC Link DEPOMOD ENV03 programme. The authors are grateful to Roy Lewis of Zeneca/Plymouth Marine Laboratory and Michael Burrows of DML for their comments on the manuscript. We would also like to thank the crew of the RV Seol Mara for their help with the sampling programme.

Literature Cited

Ackefors, H. and M. Enell. 1994. The release of nutrients and organic matter from aquaculture systems in Nordic countries. *Journal of Applied Ichthyology* 10:225–241.

Allen, C. M. 1982. Numerical simulation of contaminant dispersion in estuarine flow. *Proceedings of the Royal Society of London (A)* 381:179–194.

Amos, C. L., T. Feeney, T. F. Sutherland, and J. L. Luternauer. 1997. The stability of fine grained sediments from the Fraser River delta. *Estuarine, Coastal and Shelf Science* 45:507–524.

Black, K. D., S. Fleming, T. D. Nickell, and P. M. F. Pereira. 1997. The effects of Ivermectin, used to control sea lice on caged farmed salmonids, on infaunal polychaetes. *ICES Journal of Marine Science* 54:276–279.

Bowden, K. F. 1983. Physical Oceanography of Coastal Waters. Ellis Horwood Limited, Chichester, U.K.

Burt, T. N. and K. A. Turner. 1983. Deposition of Sewage Sludge on a Rippled Sand Bed. Report IT248. Hydraulics Research, Wallingford, U.K.

Chen, Y. S., M. C. M. Beveridge, and T. C. Telfer. 1999. Settling rate characteristics and nutrient content of the faeces of Atlantic salmon, *Salmo salar,* and the implications for modelling of waste dispersion. *Aquaculture Research* 30:395–398.

Clarke, S. and A. J. Elliot. 1998. Modelling suspended sediment concentrations in the Firth of Forth. *Estuarine, Coastal and Shelf Science* 47:235–250.

Cromey, C. J., K. D. Black, A. Edwards, and I. A. Jack. 1998. Modelling the deposition and biological effects of organic carbon from marine sewage discharges. *Estuarine, Coastal and Shelf Science* 47:295–308.

Cromey, C. J., T. D. Nickell, and K. D. Black. 1999. Economic Site Asessment through Modelling the Effects of Carbon Deposition to the Benthos from Large Scale Salmon Mariculture DEPOMOD. Report to the Natural Environment Research Council Link, Internal Report no. 214. Dunstaffnage Marine Laboratory, Oban, Argyll, U.K.

Davies, I. M., P. Smith, T. D. Nickell, and P. G. Provost. 1996. Interactions of salmon farming and benthic microbiology in sea lochs, p. 33–39. *In* K. D. Black (ed.). Aquaculture and Sea Lochs. Scottish Association for Marine Science, Oban, Argyll, U.K.

De-Jonge, V. N. and J. van den Bergs. 1987. Experiments on the resuspension of estuarine sediments containing benthic diatoms. *Estuarine, Coastal and Shelf Science* 24:725–740.

Delvigne, G. A. L. 1996. Laboratory Investigations on the Fate and Physicochemical Properties of Drill Cuttings after Discharge into the Sea. Environment and Protection Forum Report no. 2.61/202, The Physical and Biological Effects of Processed Oily Drill Cuttings. Environment and Protection Forum, London, U.K.

Dudley, R. W., V. G. Panchang, and C. R. Newell. 2000. Application of a comprehensive modeling strategy for the management of net-pen aquaculture waste transport. *Aquaculture* 187:319–349.

Dyer, K. R. 1979. Estuarine Hydrology and Sedimentation. Cambridge University Press, Cambridge, U.K.

FINDLAY, R. H. AND L. WATLING. 1997. Prediction of benthic impact for salmon net-pens based on the balance of benthic oxygen supply and demand. *Marine Ecology Progress Series* 155: 147–157.

FLEMING, G. AND R. A. WALKER. 1981. The Loch Eil Project: Simulation of the hydrology and sediment inputs to Loch Eil. *Journal of Experimental Marine Biology and Ecology* 55:103–113.

FUTAWATARI, T. AND T. KUSUDA. 1993. Modelling of suspended sediment transport in a tidal river, p. 504–519. Coastal and Estuarine Studies, No. 42. Springer-Verlag, New York.

GILLIBRAND, P. A. AND W. R. TURRELL. 1997. Simulating the dispersion and settling of particulate material and associated substances from salmon farms. Report No. 3/97. CFAS, Aberdeen, U.K.

GOWEN, R. J., N. B. BRADBURY, AND J. R. BROWN. 1989. The use of simple models in assessing two of the interactions between fish farming and the marine environment, p. 135–155. *In* R. Billard and N. de Pauw (eds.). Aquaculture—A Technology in Progress. European Aquaculture Society, Bredene, Belgium.

HANSEN, P. K., K. PITTMAN, AND A. ERVIK. 1991. Organic waste from marine fish farms—Effects on the sea bed, p. 105–119. *In* T. Mäkinen (ed.). Marine Aquaculture and Environment. Nordic Council of Ministers, Copenhagen, Denmark.

HARRIS, J. R. W., R. N. GORLEY, AND C. A. BARTLETT. 1993. ECoS Version 2—A User Manual. Plymouth Marine Laboratory, Plymouth, U.K.

HEATHERSHAW, A. D. 1988. Sediment transport in the sea, on beaches and in rivers: Part I—Fundamental principles. *Journal of Naval Research* 14:154–170.

HENDRICKS, T. J. 1987. Predicting Sediment Quality Around Outfalls. Southern Californian Coastal Water Research Project Authority, El Segunda, California.

HEVIA, M., H. ROSENTHAL, AND R. J. GOWEN. 1996. Modelling benthic deposition under fish cages. *Journal of Applied Ichthyology* 12:71–74.

HOLMER, M. AND E. KRISTENSEN. 1994. Organic matter mineralization in an organic–rich sediment: Experimental stimulation of sulfate reduction by fish food pellets. *FEMS Microbiology Ecology* 14:33–44.

KRONE, R. B. 1962. Flume Studies of the Transport of Sediment in Estuarial Shoaling Processes. University of California Hydraulic Engineering Laboratory and Sanitation Research Laboratory, Berkeley, California.

LESHT, B. M. 1979. Relationship between sediment resuspension and the statistical frequency distribution of bottom shear stress. *Marine Geology* 32:M19–M27.

LEWIS, R. AND J. O. LEWIS.1987. Shear stress variations in an estuary. *Estuarine, Coastal and Shelf Science* 25:621–635.

LUND-HANSEN, L. C., J. VALEUR, M. PEJRUP, AND A. JENSEN 1997. Sediment fluxes, resuspension and accumulation rates at two wind–exposed coastal sites and in a sheltered bay. *Estuarine Coastal Shelf Science* 44:521–531.

MARSH, J. 1995. Development of a tracer technique for the study of suspended sediment dynamics in aquatic environments. Ph.D. Dissertation, University of Plymouth, Plymouth, U.K.

MCLELLAN, H. J. 1965. Elements of Physical Oceanography. Pergamon Press, Oxford, U.K.

MEAD, C. T. 1991. A Detailed Description of SEDPLUME–RW. Random Walk Simulations of the Dispersal of Sewage Effluent and Dredged Spoil (Appendix A). Hydraulics Research Limited, Wallingford, U.K.

MEAD, C. T. AND J. G. RODGER. 1991. Random walk simulations of the dispersal of dredged spoil, p. 783–788. *In* J. Lee and D. Cheung (eds.). Environmental Hydraulics. Pergamon Press, Oxford, U.K.

MEHTA, A. J. 1984. Laboratory studies on cohesive sediment deposition and erosion, p. 427–445. *In* W. Van Leussen and J. Dronkers (eds.). Physical Processes in Estuaries. Pergamon Press, Oxford, U.K.

MICHELS, K. H. AND T. R. HEALY. 1999. Evaluation of an inner shelf site off Tauranga Harbour, New Zealand, for disposal of muddy-sandy dredged sediments. *Journal of Coastal Research* 15: 830–838.

MILLER, B. 1998. An assessment of Sediment Copper and Zinc Concentrations at Marine Caged Fish Garms in SEPA West Region. Final Report w98/04. Scottish Environment Protection Agency, Stirling, U.K.

MOON, V., W. DE LANGE, S. WARREN, AND T. HEALY. 1994. Post-disposal behaviour of sandy dredged material at an open-water, inner shelf disposal site. *Journal of Coastal Research* 10:651–662.

MORRISEY, D. J., M. M. GIBB, S. E. PICKMERE, AND R. G. COLE. 2000. Predicting impacts and recovery of marine-farm sites in Stewart Island, New Zealand, from the Findlay-Watling model. *Aquaculture* 185:257–271.

NEUMANN, G. AND W. J. PIERSON. 1966. Principles of Physical Oceanography. Prentice-Hall, Englewood Cliffs, New Jersey.

NICHOLS, M. M. 1985. Temporal variations of sediment resuspension. *Estuaries* 8:120A.

NICKELL, T. D. AND S. J. ANDERSON, 1997. Environmental Assessment of Loch Harport. Report no. UDI 911. Altra Safety and Environment Ltd., Aberdeen, U.K.

O'CONNOR, B. A. AND J. NICHOLSON. 1992. An estuarine and coastal sand transport model, p. 507–526. *In* D. Prandle (ed.). Dynamics and Exchanges in Estuaries and the Coastal Zone, Coastal and Estuarine Studies no. 40. Springer–Verlag, New York.

ODD, N. V. M. AND M. V. OWEN. 1972. A two-layer model of mud transport in the Thames estuary. *Proceedings of the Institution of Civil Engineers* 7517S:175–205.

PARTHENIADES, E. 1965. Erosion and deposition of cohesive soils. *Proceedings of the American Society of Civil Engineers* 91:105–139.

PULS, W. AND J. SÜNDERMANN. 1990. Simulation of suspended sediment dispersion in the North Sea, p. 356–372. *In* R. T. Cheng (ed.). Residual Currents and Long Term Transport, Coastal and Estuarine Studies no. 38. Springer-Verlag, New York.

RODGER, G. K., I. M. DAVIES, AND G. TOPPING. 1992. Retention of trace-metal contaminants in the sediment at an accumulating sewage-sludge disposal site. *Water Research* 26:111–120.

ROMAN, M. R. AND K. R. TENORE. 1978. Tidal resuspension in Buzzards Bay, Massachusetts. I. Seasonal changes in the resuspension of organic carbon and chlorophyll *a*. *Estuarine, Coastal and Shelf Science* 6:37–46.

SANFORD, L. P. 1992. New sedimentation, resuspension and burial. *Limnology and Oceanography* 37:1164–1178.

SANFORD, L. P. AND J. P. HALKA. 1993. Assessing the paradigm of mutually exclusive erosion and deposition of mud, with examples from upper Chesapeake Bay. *Marine Geology* 114:37–57.

SANFORD, L. P., W. PANAGEOTOU, AND J. P. HALKA. 1991. Tidal resuspension of sediments in northern Chesapeake Bay. *Marine Geology* 97:87–103.

SCOTTISH ENVIRONMENTAL PROTECTION AGENCY. 1999. Short Term Ecomonitoring Study of a Particulate Discharge. Scottish Environment Protection Agency, Stirling, Scotland.

SILVERT, W. 1992. Assessing environmental impacts of finfish aquaculture in marine waters. *Aquaculture* 107:67–79.

SILVERT, W. AND J. W. SOWLES. 1996. Modelling environmental impacts of marine finfish aquaculture. *Journal of Applied Ichthyology* 12:75–81.

SOULSBY, R. L. 1983. The bottom boundary layer of shelf seas, p. 189–266. *In* B. Johns (ed.). Physical Oceanography of Coastal and Shelf Seas. Elsevier, London, U.K.

Southern Californian Coastal Water (SCCWRP). 1992. Modification and Verification of Sediment Deposition Models. Final

Report. Southern Californian Coastal Water Research Project Authority, El Segundo, California.

TEISSON, C. 1991. Cohesive suspended sediment transport: Feasibility and limitations of numerical modelling. *Journal of Hydraulic Research* 29:755–769.

THORNE, P. D., J. J. WILLIAMS, AND A. D. HEATHERSHAW. 1989. In–situ acoustic measurements of marine gravel threshold and transport. *Sedimentology* 36:61–74.

UNCLES, R. J., R. C. A. ELLIOTT, AND S. A. WESTON. 1985. Observed fluxes of water, salt and suspended sediment in a partly mixed estuary. *Estuarine, Coastal and Shelf Science* 20:147–167.

UOTILA, J. 1991. Metal contents and spread of fish farming sludge in southwestern Finland, p. 121–126. *In* T. Mäkinen (ed.). Marine Aquaculture and Environment. Nordic Council of Ministers, Copenhagen, Denmark.

VELEGRAKIS, A. F., S. GAO, R. LAFITE, J. P. DUPONT, M. F. HUAULT, L. A. NASH, AND M. B COLLINS. 1997. Resuspension and advection processes affecting suspended particulate matter concentrations in the central English Channel. *Journal of Sea Research* 38:17–34.

WASHBURN, L., B. H. JONES, A. BRATKOVICH, T. D. DICKEY, AND M. S. CHEN. 1991. Mixing, dispersion, and resuspension in vicinity of ocean wastewater plume. *Journal of Hydraulic Engineering* 118:38–58.

WOLANSKI, E. AND R. GIBBS. 1992. Resuspension and clearing of dredge spoils after dredging, Cleveland Bay, Australia. *Water Environment Research* 64:910–914.

SOURCE OF UNPUBLISHED MATERIAL

MCKEE, D. Unpublished data. Transmissometer trials in the Firth of Lorn, Scotland. Department of Physics and Applied Physics, Strathclyde University, Glasgow, Scotland, U.K.

Received for consideration, February 2, 2000
Accepted for publication, April 5, 2002